Talanta 97 (2012) 211–217

Contents lists available at SciVerse ScienceDirect

Talanta

journal homepage: www.elsevier.com/locate/talanta

Optimization of solid-phase extraction using artificial neural networks and response surface methodology in combination with experimental design for determination of gold by atomic absorption spectrometry in industrial wastewater samples

H. Ebrahimzadeh [a,*], N. Tavassoli [b], O. Sadeghi [b], M.M. Amini [a]

[a] Department of Chemistry, Shahid Beheshti University, G. C., Tehran, 198396311, Iran
[b] Department of Chemistry, Shahr-e-Rey Branch, Islamic Azad University, P.O. Box 18735-334, Tehran, Iran

ARTICLE INFO

Article history:
Received 21 February 2012
Received in revised form
4 April 2012
Accepted 6 April 2012
Available online 12 April 2012

Keywords:
Artificial neural networks
Response surface methodology
Experimental design
Gold
Wastewater

ABSTRACT

Solid-phase extraction (SPE) is often used for preconcentration and determination of metal ions from industrial and natural samples. A traditional single variable approach (SVA) is still often carried out for optimization in analytical chemistry. Since there is always a risk of not finding the real optimum by single variation method, more advanced optimization approaches such as multivariable approach (MVA) should be applied. Applying MVA optimization can save both time and chemical materials, and consequently decrease analytical costs. Nowadays, using artificial neural network (ANN) and response surface methodology (RSM) in combination with experimental design (MVA) are rapidly developing. After prediction of model equation in RSM and training of artificial neurons in ANNs, the products were used for estimation of the response of the 27 experimental runs. In the present work, the optimization of SPE using single variation method and optimization by ANN and RSM in combination with central composite design (CCD) are compared and the latter approach is practically illustrated.

1. Introduction

As gold is so valuable and rare, it is always looked to be recovered and recycled. On the other hand, determination of this rare element is so important [1,2]. Through recent years, lots of procedures have been employed, such as electrothermal atomic absorption spectrometry (ETAAS) [3,4], inductively coupled plasma optical emission spectroscopy (ICP-OES) [5,6], inductively coupled plasma mass spectroscopy [7,8] and flame atomic absorption spectroscopy [9,10]. Although ICP-OES and ETAAS are more sensitive and procedures that used them have better figures of merit, flame atomic absorption spectrometry (FAAS) is one of the most popular analytical tools for the determination of low levels of heavy metals due to its conventional handling and low expense [11,12]. Nevertheless, low insufficient sensitivity of instrument and matrix interference are two indispensable disadvantages of FAAS [13]. However, these problems can be easily resolved by the preconcentration technique due to the possibility of removing the sample matrix and increasing sensitivity [14]. For this reason, several methods have been applied for preconcentration and separation of trace concentration of gold according to the nature of the samples and the concentrations of the analyte. They include ion exchange [15], coprecipitation [16], solvent extraction [17] and adsorption on a solid phase [18–20]. Among them, solid-phase extraction has attracted more attention as it is more capable and conventional in preconcentration [21]. A wide range of solid phases for extraction of gold has been proposed and used: active carbon [22], polyurethane foam [23], surfactant coated silica gel [24–26], and mesoporous silica [27,28]. Among these various solids, mesoporous silica has gained much importance for metal ion enrichment due to high surface area (up to 1300 $m^2 g^{-1}$) that causes high adsorption capacity, chemical and mechanical stabile properties which never shrink or expand and also easy synthesis procedure [29]. However, still there is a problem, mesoporous silica could not act so perfect without modifications. Modification improves their performance as it could increase selectivity and adsorption ability.

Traditional single variation method is not a confident method for finding real optimums, so more advanced optimization approaches such as the multivariable approach (MVA) should be applied. Applying MVA optimization can save time and chemical and also decreases analytical cost. Nowadays, the use of artificial neural network (ANN) and response surface methodology (RSM) in combination with experimental design (MVA) is rapidly developing [30–35].

* Corresponding author. Tel.: +98 21 29902891; fax: +98 21 22403041.
E-mail address: h-ebrahim@sbu.ac.ir (H. Ebrahimzadeh).

0039-9140/$ - see front matter © 2012 Elsevier B.V. All rights reserved.
http://dx.doi.org/10.1016/j.talanta.2012.04.019

In this work, novel pyridine functionalized MCM-48 mesoporous silica has been used as a powerful adsorbent for solid-phase extraction of gold ions. For the first time, artificial neural network was applied for solid-phase extraction to determine gold ions, and results were compared with response surface methodology and single variation method. This system has been applied successfully in real samples such as industrial water samples and the accuracy of these methods was also confirmed by some standard materials.

2. Experimental

2.1. Reagents and materials

All reagents were of analytical grade and used as received standard solution of gold with concentration of 1000 μg $mL^{-1}$and HCl and HNO_3 were purchased from Merck (Darmstadt, Germany). The working solutions of gold were prepared by diluting appropriate amounts of the stock solutions with buffer solutions. A Milli-Q (Millipore, Bedford, MA, USA) purification system was employed to provide the deionized water needed to prepare all the required solutions. MCM-48 mesoporous silica was prepared according to the previously reported procedures [36] and the mesoporous structure was confirmed by low-angle X-ray diffraction. For synthesis of N-(3-(triethoxysilyl)propyl)picolonicamide (TPP), in a 250 mL two-neck round-bottom flask equipped with a magnetic stir bar and a reflux condenser, 2.0 g (16 mmol) of 4-pyridine carboxylic acid was suspended in 100 mL of dry CH_2Cl_2 under nitrogen atmosphere. To this solution 5 mL of oxalylchloride was slowly added from a dropping funnel and the mixture was stirred for 8 h. Then CH_2Cl_2 was removed under reduced pressure, and the residue was suspended again in 100 mL of dry CH_2Cl_2. After addition of 7 mL triethylamine to reaction mixture, 4.0 g 3-aminopropyltrimethoxysilane was slowly added. The reaction mixture was stirred at room temperature for further 4 h. The mixture was suspended in water to remove impurities; then the organic phase separated and the solvent was removed under reduced pressure to obtain brownish viscose oil [37].

For preparation of pyridine functionalized MCM-48, 1.0 g of MCM-48 was suspended in 50 mL toluene and the mixture was stirred for 1 h and then 2.0 g of TPP was added and refluxed for 2 h. The white-brownish solid was removed by filtration and was washed with toluene and ethanol and then dried at room temperature. Synthesis of MCM-48 and pyridine-functionalized material was confirmed by IR spectroscopy, low-angle X-ray diffraction and elemental analysis. Elemental analysis of 2-Py-MCM-48 sample gave pyridine concentration of 1.92 mmol g^{-1}. A schematic diagram of modified MCM-48 with pyridine is shown in Fig. 1.

2.2. Optimization

In this study, effects of flow rate, type, concentration and volume of eluent on the recovery of gold desorption from functionalized MCM-48 silica were investigated. The levels of four independent variables were selected, based on the previous data and preliminary works [27]. Totally, 27 experimental points were defined using central composite design (CCD). This major class of designs has two parts: a cube and a star. The cube portion corresponds to a factorial screening design and the star portion of the design consists of an additional set of points arranged at equal distances from the center of the cube on radii that pass through the center point on each face of the cube.

For modeling and prediction of recovery of desorbed gold ions response surface methodology (RSM) and artificial neural network (ANN) were used. RSM is a collection of mathematical and statistical techniques used to define the relationship between the response and the variables. RSM is mainly used for optimization of the effective parameters and scaling up the condition. In addition, prediction of model equation is one of the steps of RSM optimization procedure. In order to estimate the response at different levels of variables, model equation was calculated. Therefore, the values of variables and the response were used for prediction of model equations.

Parallel systems of simple processing elements, neurons, are interconnected to produce artificial neural network. In the present study, feed forward, multi-layer perceptions (MLP) type of ANN was used to predict the optimum conditions. Training of the ANN was accomplished through the back-propagation algorithm in MLP, which is the most commonly used in supervised MLP. Different network architectures were tested and the best prediction was obtained for a network of one hidden layer with 50 neurons. The transfer function was sigmoid function. In the training procedure, the information is processed in the forward direction from input layer to hidden and then output layer obtained as the output of the network.

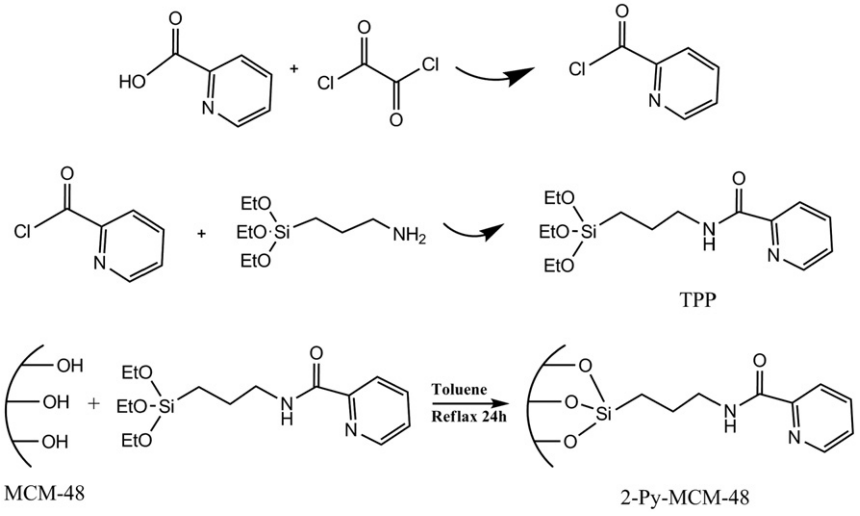

Fig. 1. Functionalization of MCM-48 mesoporous silica by TPP.

The data were processed using Matlab7.80 for artificial neural network and Stat Graphics Plus package, version 5.1, for experimental design matrix and data analysis.

2.3. Sample preparation

Water samples were obtained from tap water (Tehran, Iran) and jewelry manufacturing firms (Tehran, Iran). After filtering water samples through 0.45 μm pore size nylon, they were collected in cleaned polyethylene bottles. Three mine stones from gold mineral with certified concentrations of gold, which were reported by Geological Survey of Iran, were obtained. Mineral samples were digested in an 8 mL mixture of 5% aqua regia with the assistance of a microwave digestion system. Digestion was carried out for 2 min at 250 W, 2 min at 0 W, 6 min at 250 W, 5 min at 400 W and 8 min at 550 W, and the mixture was then vented for 8 min. The residue from this digestion, as well as a control digestion, was then diluted with deionized water. Finally, the proposed method was applied to separate and preconcentrate gold ions in optimum conditions which were obtained by each optimized method from the aforementioned water samples.

3. Result and discussion

In the present study, artificial neural network and response surface methodology in combination with experimental design were applied for determination of gold in industrial waste water samples. In addition, after optimization of desorption process by ANN and RSM, two models were compared and the results have been presented. In this context, gold ions were adsorbed by functionalized MCM-48 in optimum condition. Similar to the previous study for gold extraction by MCMs, two effective factors on adsorption process, pH and sample flow rate were optimized [27]. According to the previous study adsorption factors were optimized and at pH=3 and flow rate of 12 mL min^{-1}, the adsorption recovery of more than 99.5% was found [27].

The parameters for gold desorption were flow rate, type, concentration and volume of eluent. Those parameters for desorption of gold ions by functionalized MCM-48 were optimized in three ways, one factor at a time, CCD-RSM and CCD-ANN. Finally, three methods were compared with each other.

3.1. Single variable approach

According to the previous studies [27], all parameters such as type, concentration, volume and flow rate of eluent were optimized.

3.2. Multivariation approach

According to MVA, all variables should be changed at the same time. In the present work, central composite design (CCD) was applied for four parameters to design an experiment. The obtained data were used for modeling, using response surface methodology and neural networks.

Previous studies have shown that four parameters for elution process have to be considered during SPE optimization [27]. Desorption recovery depends on concentration of thiourea (X_1), concentration of HCl (X_2), elution flow-rate (X_3) and eluent volume (X_4). The domain of variation for each factor was determined based on knowledge of the system and acquired from initial experimental trials (Table 1). A total of 27 experiments were carried out; X_1, X_2, X_3 and X_4 variables and also their domains are shown in Table 2.

Table 1
Effective factors and factor levels for desorption of gold ions on functionalized MCM-48.

Factors	Levels				
	Lowest −1.62	Low −1	Center 0	High +1	Highest +1.62
(A) Flow rate (mL min^{-1})	1	2	3	4	5
(B) HCl concentration (mol L^{-1})	0.25	1.5	2.75	4	5.25
(C) Thiourea concentration (mol L^{-1})	0	0.3	0.6	0.9	1.2
(D) Eluent volume (mL)	1.5	5	8.5	12	15.5

Table 2
Central composite design matrix for the optimization of the desorption of gold on functionalized MCM-48.

Run	Flow rate (mL min^{-1})	HCl concentration (mol L^{-1})	Thiourea concentration (mol L^{-1})	Eluent volume (mL)	Recovery (%)
1	4	1.5	0.9	12.0	89.4
2	4	4.0	0.9	5.0	50.3
3	4	1.5	0.3	5.0	29.6
4	2	4.0	0.9	12.0	99.2
5	2	1.5	0.9	5.0	57.7
6	4	4.0	0.3	12.0	85.1
7	3	2.75	0.6	8.5	94.5
8	2	1.5	0.3	12.0	78.0
9	2	4.0	0.3	5.0	58.6
10	4	1.5	0.3	12.0	48.6
11	4	1.5	0.9	5.0	46.2
12	2	1.5	0.3	5.0	38.1
13	4	4.0	0.3	5.0	43.5
14	2	4.0	0.9	5.0	74.2
15	2	4.0	0.3	12.0	98.9
16	3	2.75	0.6	8.5	94.8
17	4	4.0	0.9	12.0	99.6
18	2	1.5	0.9	12.0	98.5
19	3	2.75	0.6	1.5	3.2
20	3	5.25	0.6	8.5	99.4
21	3	0.25	0.6	8.5	20.6
22	3	2.75	0.6	15.5	99.8
23	5	2.75	0.6	8.5	82.4
24	3	2.75	0.0	8.5	53.2
25	3	2.75	1.2	8.5	99.7
26	1	2.75	0.6	8.5	99.8
27	3	2.75	0.6	8.5	95.4

3.2.1. CCD-RSM

The extraction condition was optimized by using response surface methodology. Experiments required for optimizing four factors in this design are shown in Table 2. The significance of the variables in the desorption process was evaluated using Pareto's chart. As shown in Fig. 2, at the 5% significance level all four factors are important, volume of elution has the most positive effect on the desorption recovery and flow rate of elution is the only negative effect between all main factors. This design includes the possibility of evaluating cross-effects between variables without the need of performing additional experiments. For gold desorption yield Y is as follows:

$$Y = -122.498 - 15.4739A + 5.38083C + 48.7062B + 119.492\mathrm{D} - 1.30833A^2 - 1.59AB - 3.16667AC + 0.5AD - 5.81333B^2 - 13.5333BC + 0.731429BD - 55.2315C^2 + 3.29762CD - 0.914966D^2 \quad (1)$$

After identifying the most significant variables, response surface methodology was used to find optimum condition for the

best recovery. The summary of analysis, which has been shown by the contour plot and response surface plot, is illustrated in Fig. 3. For this reason, the R-squared statistic has been adjusted to 98.5%, which indicates that the model could explain 98.5% of the variability of the mean recovery of the gold desorption on functionalized MCM-48. As can be seen in Fig. 3, by increasing volume and decreasing flow rate, quantitative recovery has been obtained. Moreover, it seems that optimum condition can be obtained more precisely by using artificial neural network rather than response surface methodology.

3.2.2. CCD-ANN

Four factors, flow rate, HCl concentration, thiourea concentration, and eluent volume, were used as each unit of input layer. The output layer was composed of the recovery of desorption process as a response variable. A set of factors such as number of neurons in hidden layer, irritation, and training algorithm was optimized to train and feed into the computer.

Back propagation was applied as a suitable network searching for this work. In order to select the best learning step, seven algorithms were tested in the same condition. For this reason, output values predicted by ANN were plotted against the corresponding observed values. Linear regression analysis was used to calculate the gradient (m), intercept (c) and goodness of fit (R^2) in order to investigate the efficiency of each training algorithm for the experiment. The results for each algorithm are shown in Table 3. As can be seen, the amount of R^2 is more than 0.9 for three algorithms of CGB, BFG and OSS, which shows that the models will be predictive if those three algorithms apply for training step. The comparison of the correlation coefficient shows a clear superiority of CGB, BFG and OSS compared to other algorithms. Afterward, three algorithms were tested again and the obtained mean square errors were used to compare three algorithms together. As can be seen in Table 4, the MSE values are obtained as 85.31 and 44.21 for OSS and RP, respectively. The least amount of MSE is obtained by CGB learning algorithm equal to 21.66, which shows its efficiency for training step. Therefore, CGB was applied as learning algorithm for further study.

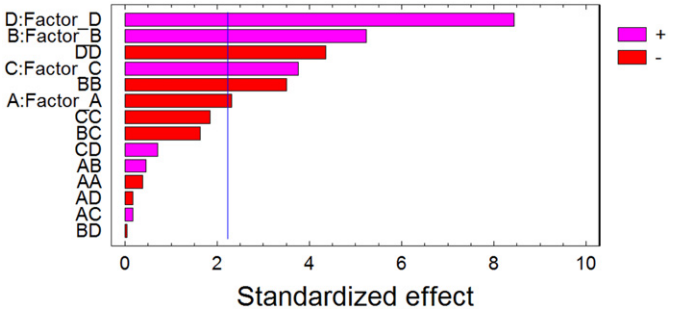

Fig. 2. Pareto chart for desorption process, which shows the significance of four factors: (A) flow rate, (B) HCl concentration, (C) thiourea concentration, and (D) volume of elution.

Table 3
Comparison of m, b and R obtained by seven kinds of training algorithms.

	CGB[a]	RP[b]	CGP[c]	CGF[d]	Lm[e]	BFG[f]	OSS[g]
M[h]	0.9480	0.9340	0.1450	0.1124	0.3829	0.7446	0.9446
B[i]	2.4841	3.6111	55.3437	58.4288	43.9563	12.6367	2.6367
R[j]	0.9939	0.9932	0.7082	0.7342	0.6335	0.8914	0.9914

Condition of ANN: number of inputs: 4, number of hidden layer: 1, number of neurons: 10.

[a] Conjugate gradient with Powell/Beale restarts.
[b] Resilient backpropagation.
[c] Polak–Ribiere conjugate gradient.
[d] Fletcher–Powell conjugate gradient.
[e] Levenberg–Marquardt.
[f] BFGS quasi-Newton.
[g] One step secant.
[h] Slope.
[i] Intercept.
[j] Regression coefficient.

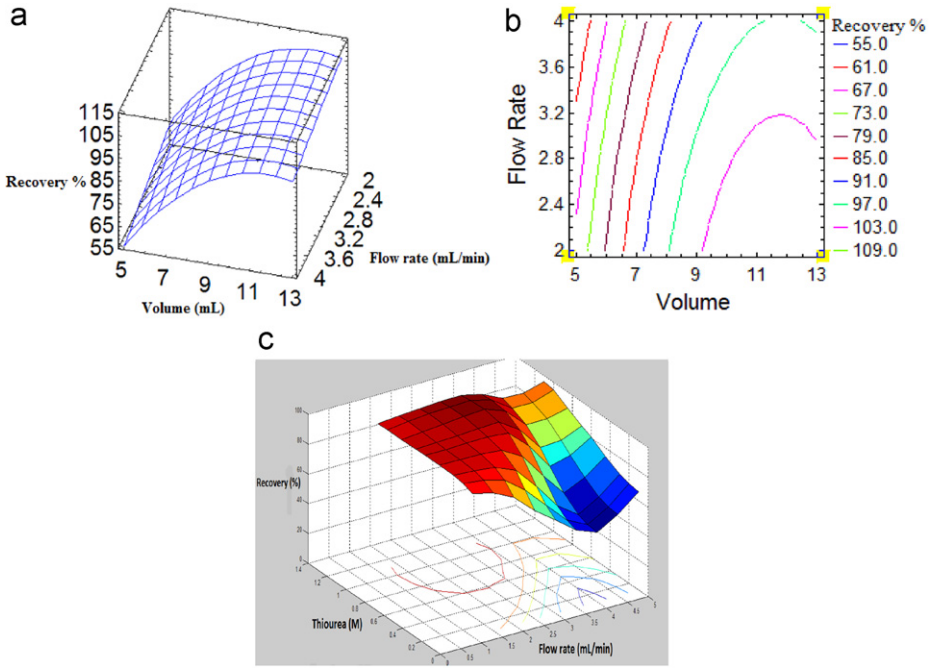

Fig. 3. Response surfaces and contour plot, (a) response surface for the recovery (%) as a function of volume of eluent (mL) and flow rate (mL/min) obtained by experimental design methodology, (b) contour plot for flow rate (mL/min) as a function of eluent volume (mL) obtained by experimental design methodology, (C) response surface for the recovery (%) as a function of concentration of eluent (mol/mL) and flow rate (mL/min) obtained by experimental design methodology. ANN condition: training algorithm: CGB, number of neurons: 50, number of inputs: 4, number of hidden layer, number of irritations: 400.

Choosing the number of hidden layers is difficult, but typically one hidden layer is used in a network. In the present work, one hidden layer is used because a significant improvement in performance by increasing the number of hidden layers is not observed. Several iterations were conducted with different numbers of epochs and neurons of hidden layer to determine the optimal ANN structure. The optimum number of neurons or epochs in the hidden layer was iteratively determined by changing the number of neurons or epochs. It started with 2 neurons and 10 epochs and increased later. The learning curve for training is given in Fig. 4.

As can be found in Fig. 4, mean square error (MSE) decreases initially and then it becomes almost constant. Therefore, the least

Table 4
Comparison of mean square errors obtained by three kinds of training algorithms.

Training algorithm	RP[a]	OSS[b]	CGB[c]
MSE[d]	44.21	85.31	21.66

Condition of ANN: number of inputs: 4, number of hidden layer: 1, number of neurons: 10.

[a] Resilient backpropagation.
[b] One step secant.
[c] Polak–Ribiere conjugate gradient.
[d] Mean square error.

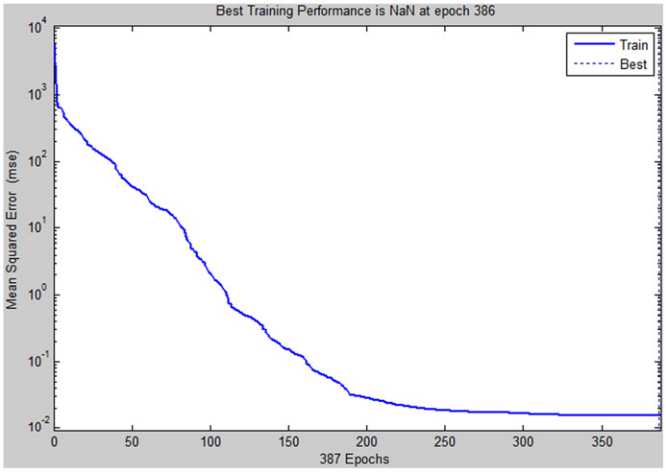

Fig. 4. Learning curves for training set. Condition for ANN: training algorithm: CGB, number of inputs: 4, number of hidden layer: 1.

Table 5
Effect of the number of neurons on mean square error, mean absolute error and *R*.

Neurons	MSE[a]	MAE[b]	*R*[c]
3	183.4702	8.9439	0.8787
5	442.6573	16.7793	0.6736
10	602.92	21.6630	0.8029
20	85.5744	6.6093	0.9458
30	0.1628	0.2550	0.9999
40	0.0306	0.0860	1.0000
50	0.0156	0.0386	1.0000
60	0.0255	0.0725	1.0000
70	0.0156	0.0385	1.0000

Condition of ANN: number of inputs: 4, number of hidden layer: 1, training algorithm: CGB.

[a] Mean square error.
[b] Mean absolute error.
[c] Regression coefficient.

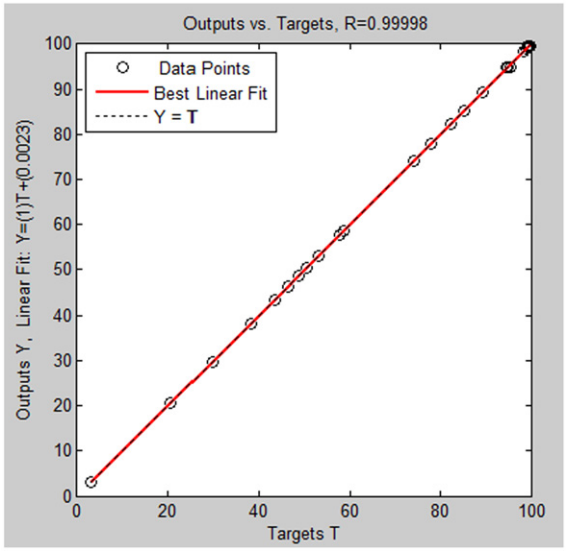

Fig. 5. Experimental and ANN predicted recovery for gold desorption for the training set. Condition for ANN: training algorithm: CGB, number of neurons: 50, number of inputs: 4, number of hidden layer: 1, number of irritations: 400.

Table 6
Optimized conditions obtained by three different optimization methods.

Optimization method	Flow rate (mL min^{-1})	HCl concentration (mol L^{-1})	Thiourea concentration (mol L^{-1})	Eluent volume (mL)
SVA	**2.0**	**3.0**	**1.0**	**10.0**
CCD-RSM	**1.5**	**3.3**	**0.8**	**10.5**
CCD-ANN	**1.9**	**3.0**	**0.9**	**8.1**

Condition of ANN: training algorithm: CGB, number of neurons: 50, number of inputs: 4, number of hidden layer: 1, number of irritations: 400.

Table 7
Measured and estimated responses by RSM and ANN for ten random experiments

Run	Flow rate	HCl	Thiourea	Volume	RSM	ANN	Experiment
1	3	2.5	0.5	4	46.81388	38.551	40.3
2	2	1.5	0.2	6	31.04676	32.6366	32.5
3	2	3.0	1.0	6	83.4723	90.0921	91.2
4	1	2.5	0.9	7	93.09602	102.3034	99.4
5	1	3.5	0.7	13	112.7954	99.7627	99.7
6	2	1.5	0.1	10	34.48466	55.4565	51.9
7	3	1.5	0.5	8	64.93298	59.6421	60.6
8	2	2.0	0.3	8	64.53673	55.9536	57.1
9	3	4.0	0.4	5	61.32669	48.762	52.1
10	2	3.0	0.8	11	113.646	99.6997	99.8

Condition of ANN: training algorithm: CGB, number of neurons: 50, number of inputs: 4, number of hidden layer: 1, number of irritations: 400.

Table 8
Comparison of mean absolute and square errors obtained of two optimized methods.

Error	ANN	RSM
MAE[a]	0.17	−2.55
MSE[b]	3.87	96.97

Condition of ANN: training algorithm: CGB, number of neurons: 50, number of inputs: 4, number of hidden layer, number of irritations: 400.

[a] Mean absolute error.
[b] Mean square error.

MSE value was obtained with 50 neurons and 400 epochs in the hidden layer. The results are shown in Table 5 and Fig. 4. Therefore, the optimal structure of the network with 50 neurons in the hidden layer and 400 epochs was applied for further prediction (4:50:1), which 4 shows the number of factors, 50 is related to the number of neurons in hidden layer and 1 is the number of yield. The sigmoid and linear functions were used as the transfer functions for the hidden and output layer nodes, respectively. During the training process, the values of weights between individual neurons were assigned. To determine how a neural network is performing during iterative training, the value of errors was calculated.

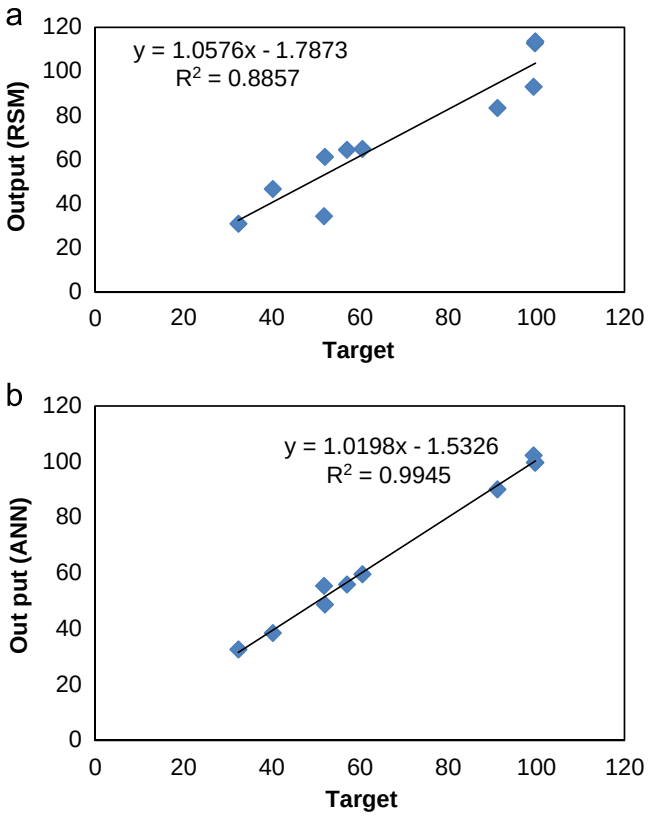

Fig. 6. Experimental and (a) RSM, (b) ANN predicted recovery for the testing set. Condition for ANN: training algorithm: CGB, number of neurons: 50, number of inputs: 4, number of hidden layer: 1, number of irritations: 400.

The trained network was used to estimate the response of 27 experimental points. R^2 between actual and estimated responses was determined as 0.999 (Fig. 5). The optimum condition is obtained by artificial neural network as optimized method is shown in Table 6. As can be seen, there are more than one point with quantitative recovery (>99). However, the optimum condition with the lowest amount of eluent volume is selected to obtain the higher concentration factor. The summary of the optimum conditions which is obtained by three different optimization methods is listed in Table 6.

3.3. Comparative study of the ANN and RSM modeling

After modeling, ten experiments were designed randomly with Matlab programming, and the predicted recoveries obtained by ANN and RSM were compared with SVA results (Table 7). Mean absolute and square error data is shown in Table 8. As can be seen, the values of MAE and MSE are obtained as 96.97 and −2.55 for RSM, which are too large than those of ANN. Therefore, calculated data by ANN model prediction are more similar to the experiments results those of RSM predicted results. In addition, the predicted and experimental recoveries for desorption of gold ions on functionalized MCM-48 by ANN and RSM are shown in Fig. 6. There was a good agreement between the ANN predictions and experimental data with a correlation coefficient of 0.9945, whereas this amount decreases to 0.8857 for RSM methodology. Therefore, artificial neural network can be accepted

Table 9
Data of univariate calibration for gold desorption on MCM-48 optimized by different methods.

Optimized method	Number of experiments	r^2	Limit of detection (ng mL^{-1})	Concentration factor	Recovery (%)	RSD[a] (%)
SVA	10	0.997	0.076	857	99.4	0.9
CCD-RSM	10	0.999	0.084	830	99.6	0.9
CCD-ANN	10	0.998	0.060	1050	99.3	1.4

Condition: SVA: flow rate: 2.0 mL min^{-1}, HCl concentration: 3.0 mol L^{-1}, thiourea concentration: 1.0 mol L^{-1}, volume: 10.0 mL; CCD-RSM: flow rate: 1.5 mL min^{-1}, HCl concentration: 3.3 mol L^{-1}, thiourea concentration: 0.8 mol L^{-1}, volume: 10.5 mL; CCD-ANN: flow rate: 1.9 mL min^{-1}, HCl concentration: 3.0 mol L^{-1}, thiourea concentration: 0.9 mol L^{-1}, volume: 8.1 mL.

[a] Relative standard deviation for 50 ng mL^{-1}.

Table 10
Determinationof gold in mine stones, for accuracy test of the optimized methods ($N=4$).

Samples	Certified value (μg g^{-1})	Found value (μg g^{-1})			Recovery (%)			Standard deviation			Zero hypothesis T-test ($p=0.05$)		
		SVA	RSM	ANN	SVA	RSM	ANN	SVA	RSM	ANN	SVA	RSM	ANN
Mine stone 1	1.100	1.018	1.119	1.040	92.5	101.7	94.5	1.3	0.9	0.9	Y	Y	Y
Mine stone 2	0.600	0.607	0.641	0.611	101.2	106.8	101.8	0.8	2.1	1.1	Y	Y	Y
Mine stone 3	6.400	6.290	6.410	6.327	98.3	100.1	98.8	1.9	1.6	1.1	Y	Y	Y

Condition: SVA: flow rate: 2.0 mL min^{-1}, HCl concentration: 3.0 mol L^{-1}, thiourea concentration: 1.0 mol L^{-1}, volume: 10.0 mL; CCD-RSM: flow rate: 1.5 mL min^{-1}, HCl concentration: 3.3 mol L^{-1}, thiourea concentration: 0.8 mol L^{-1}, volume: 10.5 mL; CCD-ANN: flow rate: 1.9 mL min^{-1}, HCl concentration: 3.0 mol L^{-1}, thiourea concentration: 0.9 mol L^{-1}, volume: 8.1 mL.

Table 11
Recovery and precision of the determination of gold in various samples.

Samples	Real sample (ng mL^{-1})			Added (ng mL^{-1})	Found (ng mL^{-1})			Recovery (%) ± standard deviation		
	SVA	RSM	ANN		SVA	RSM	ANN	SVA	RSM	ANN
Distilled water	ND	ND	ND	2.000	1.986	1.988	1.988	99.3 ± 0.9	99.4 ± 0.9	99.4 ± 1.4
Tap water	ND	ND	ND	2.000	1.960	1.984	1.984	98.0 ± 1.2	97.5 ± 1.1	99.2 ± 1.3
Waste water	49.7	51.1	49.9	50.00	96.50	99.78	98.00	96.8 ± 1.8	98.7 ± 2.3	98.1 ± 2.0

Condition: SVA: flow rate: 2.0 mL min^{-1}, HCl concentration: 3.0 mol L^{-1}, thiourea concentration: 1.0 mol L^{-1}, volume: 10.0 mL; CCD-RSM: flow rate: 1.5 mL min^{-1}, HCl concentration: 3.3 mol L^{-1}, thiourea concentration: 0.8 mol L^{-1}, volume: 10.5 mL; CCD-ANN: flow rate: 1.9 mL min^{-1}, HCl concentration: 3.0 mol L^{-1}, thiourea concentration: 0.9 mol L^{-1}, volume: 8.1 mL.

as a more precise method than response surface methodology for modeling of desorption of gold ions on MCM-48.

3.4. Applications of the optimized conditions

SPE is an efficient preconcentration method in analysis extraction of heavy metals. The optimal conditions of SPE found by SVA and MVA (CCD-RSM and CCD-ANN) were applied and LOD of gold extraction were obtained as 0.076, 0.084 and 0.060 for SVA, CCD-RSM and CCD-ANN, respectively (Table 9). For this reason, calibration curves were achieved and LOD values were calculated according to the calibration curve from $C_{LOD} = kS_b/m$, where the numerical factor, k, equals 3.

Three certified reference materials were used for validation of the proposed method. As can be found in Table 10, a good correlation was obtained between the estimated content and the one found by the present method (with all obtained conditions by SVA and MVA). Therefore, the optimized method by ANN or RSM can be used as a confident method for extraction and determination of gold by functionalized MCM-48 in different kinds of samples.

3.5. Determination of gold in real industry sample

In the present method, functionalized MCM-48 was used as a selective sorbent for gold extraction at pH of 3 and was applied as solid phase to reduce the undesirable effect of complex matrices of real samples. Table 11 shows the gold recovery in industrial samples.

4. Conclusions

The advantages of artificial neural network in comparison with single variation analysis and response surface methodology were shown. By using central composite design the number of required experiments was obtained to be more than two times lower than that of single variation approach. Applying CCD decreases the time of analysis and experiment expense without any obvious reduction in efficiency. Moreover, it was shown that optimization using ANN's is more accurate in comparison with RSM met. Although by applying AAN and RSM no obvious improvement in selectivity has been obtained, but saving in time, cost and solution consumption are three important factors, which improve in this way. Moreover, limit of detection improves by using ANN, which can be informed by reported LOD values [27].

References

[1] M. Shamsipur, M. Ramezani, Talanta 75 (2008) 294–300.
[2] I.S. Kwaka, Y. Yun, Bioresour. Technol. 101 (2010) 8587–8592.
[3] I.D. Calle, F. Pena-Pereira, N. Cabaleiro, I. Lavilla, C. Bendicho, Talanta 84 (2011) 109–115.
[4] Sh. Kagaya, D. Takata, T. Yoshimori, T. Kanbara, K. Tohda, Talanta 80 (2010) 1364–1370.
[5] L. Tavakoli, Y. Yamini, H. Ebrahimzadeh, A. Nezhadali, Sh. Shariati, F. Nourmohammadian, J. Hazard. Mater. 152 (2008) 737–743.
[6] S.S. Jibrin, Ch. Huang, J. Li, N. Zhang, B. Hu, Geostand. Geoanal. Res. 33 (2009) 469–476.
[7] R. Kovacs, S. Schlosser, S.P. Staub, A. Schmiderer, E. Pernicka, D. Günther, J. Anal. At. Spectrom. 24 (2009) 476–483.
[8] A. Scheffer, C. Engelhard, M. Sperling, W. Buscher, Anal. Bioanal. Chem. 390 (2008) 249–252.
[9] H.B. Senturk, A. Gundogdu, V.N. Bulut, C. Duran, M. Soylak, L. Elcid, M. Tufekci, J. Hazard. Mater. 149 (2007) 317–323.
[10] G. Chakrapani, P.L. Mahant, D.S.R. Murty, B. Gomathy, Talanta 53 (2001) 1139–1147.
[11] M. Bagheri, M.H. Mashhadizadeh, S. Razee, Talanta 60 (2003) 839–844.
[12] D.Q. Hung, O. Nekrassova, R.G. Compton, Talanta 64 (2004) 269–277.
[13] J.E. Renew, Ch. Huang, J. Chromatogr. A 1042 (2004) 113–121.
[14] T.P. Rao, S. Daniel, J.M. Gladis, TrAC, Trends Anal. Chem. 23 (2004) 28–35.
[15] T.E. Green, S.L. Law, W.J. Campbell, Anal. Chem. 42 (1970) 1749–1753.
[16] H. Niskavaara, E. Kontas, Anal. Chim. Acta 231 (1990) 273–282.
[17] M.B. Mooiman, J.D. Miller, Hydrometallurgy 16 (1986) 245–261.
[18] M. Tuzen, K.O. Saygi, M. Soylak, J. Hazard. Mater. 156 (2008) 591–595.
[19] Q. Hu, X. Yang, Zh. Huang, J. Chen, G. Yang, J. Chromatogr. A 1094 (2005) 77–82.
[20] L. Elci, D. Sahan, A. Basaran, M. Soylak, Environ. Monit. Assess. 132 (2007) 331–338.
[21] M. Hennion, J. Chromatogr. A 856 (1999) 3–54.
[22] M. Ghaedi, A. Shokrollahi, A.H. Kianfar, A.S. Mirsadeghi, A. Pourfarokhi, M. Soylak, J. Hazard. Mater. 154 (2008) 128–134.
[23] I. Liška, J. Krupčíik, P.A. Leclercq, J. High Resolut. Chromatogr. 12 (1989) 577–590.
[24] R. Liu, P. Liang, Anal. Chim. Acta 604 (2007) 114–118.
[25] S.S. Bozkurt, M. Merdivan, Environ. Monit. Assess. 158 (2009) 15–21.
[26] Ch. Huang, B. Hu, Spectrochim. Acta Part B 63 (2008) 437–444.
[27] H. Ebrahimzadeh, N. Tavassoli, O. Sadeghi, M.M. Amini, M. Jamali, Microchim. Acta 172 (2011) 479–487.
[28] H. Ebrahimzadeh, N. Tavassoli, M.M. Amini, Y. Fazaeli, H. Abedi, Talanta 81 (2010) 1183–1188.
[29] S. Chytil, L. Haugland, E.A. Blekkan, Micro. Meso. Mater. 111 (2008) 134–142.
[30] A.T. Tran, R.V. Hyne, F. Pablo, et al., Talanta 71 (2007) 1268–1275.
[31] M.A. Bezerra, R.E. Santelli, E.P. Oliveira, L.S. Villar, L.A. Escaleira, Talanta 76 (2008) 965–977.
[32] D. Bingol, M. Kulcu, Analyst 136 (2011) 4036–4044.
[33] M.G. Moghaddam, M. Khajeh, Food Sci. Nutr. 2 (2011) 803–808.
[34] R. Nelofer, R.N. Ramanan, J. Ind. Microbiol. Biotechnol. 39 (2012) 243–254.
[35] D. Bingöl, M. Hercan, S. Elevli, E. Kilic, Bioresour. Technol. (2012) http://dx.doi.org/10.1016/j.biortech.2012.02.084.
[36] J. Hoogboom, P.M.L. Garcia, M.B. Otten, J.A.W. Elemans, J. Sly, S.V. Lazarenko, T. Rasing, A.E. Rowan, R.J.M. Nolte, J. Am. Chem. Soc. 127 (2005) 11047–11052.
[37] K. Schumacher, M. Grun, K.K. Unger, Micropor. Mesopor. Mater. 27 (1999) 201–206.